Vascular Endothelial Growth Factor (VEGF) and Platelet (PF-4) Factor 4 Inputs Modulate Human Microvascular Endothelial Signaling in a Three-Dimensional Matrix Migration Context*[S]

Ta-Chun Hang‡¶, Nathan C. Tedford‡¶, Raven J. Reddy‡, Tharathorn Rimchala‡, Alan Wells§, Forest M. White‡, Roger D. Kamm‡, and Douglas A. Lauffenburger‡‖

The process of angiogenesis is under complex regulation in adult organisms, particularly as it often occurs in an inflammatory post-wound environment. As such, there are many impacting factors that will regulate the generation of new blood vessels which include not only pro-angiogenic growth factors such as vascular endothelial growth factor, but also angiostatic factors. During initial postwound hemostasis, a large initial bolus of platelet factor 4 is released into localized areas of damage before progression of wound healing toward tissue homeostasis. Because of its early presence and high concentration, the angiostatic chemokine platelet factor 4, which can induce endothelial anoikis, can strongly affect angiogenesis. In our work, we explored signaling crosstalk interactions between vascular endothelial growth factor and platelet factor 4 using phosphotyrosine-enriched mass spectrometry methods on human dermal microvascular endothelial cells cultured under conditions facilitating migratory sprouting into collagen gel matrices. We developed new methods to enable mass spectrometry-based phosphorylation analysis of primary cells cultured on collagen gels, and quantified signaling pathways over the first 48 h of treatment with vascular endothelial growth factor in the presence or absence of platelet factor 4. By observing early and late signaling dynamics in tandem with correlation network modeling, we found that platelet factor 4 has significant crosstalk with vascular endothelial growth factor by modulating cell migration and polarization pathways, centered around P38α MAPK, Src family kinases Fyn and Lyn, along with FAK. Interestingly, we found EphA2 correlational topology to strongly involve key migration-related signaling nodes after introduction of platelet factor 4, indicating an influence of the angiostatic factor on this ambiguous but generally angiogenic signal in this complex environment. ***Molecular & Cellular Proteomics 12: 10.1074/mcp.M113.030528, 3704–3718, 2013.***

Angiogenesis, the formation of blood vessels from pre-existing blood vessels, is a complex process essential for repairing injured tissue or supporting tissue growth. A great deal of work has been done to focus on understanding this phenomenon as it occurs *in vivo*, in particular with regard to its roles in embryonic development (1–5). In contrast to embryonic development, adult angiogenesis and inflammation are closely related phenomena that occur *in vivo* in a number of physiologically relevant processes. Inflammation lies at the crux of multiple physiological events in biological systems that precede the induction of angiogenesis: wound healing (6–8), chronic wounds (8), inflammatory disorders (9, 10), and cancer (9, 11, 12).

Inflammatory reactions also confound tissue engineered implantable three-dimensional constructs that provide innovative clinical treatments of various diseases and injuries (13–17). As complex tissues become developed for applications in clinical trials, tissue vascularization for constructs of considerable size and volume is required for their survival (18, 19). Once implanted, these constructs will also experience significant inflammatory responses within their host's local milieu (20, 21). These circumstances demonstrate the necessity for understanding the interactions between inflammation and angiogenesis, such as the development of predictive models (22). Elucidating specific intracellular mechanisms can provide insight for novel approaches in treatment of diseases as well as predicting responses to artificially engineered tissues.

Recently, studies have shown that chemokines, which play a central role in inflammation, can influence the outcomes of angiogenesis (23–26) by promoting new blood vessel growth (*e.g.* CXCL1–3, CXCL5–8, CXCL12) or inhibiting its formation altogether (*e.g.* CXCL4, CXCL9–11, CXCL13) (26). In particular, a large body of information is available on platelet factor 4 (PF-4/CXCL4) and its ability to inhibit and even induce regression of angiogenesis. PF-4 is found throughout the adult body, at roughly 0.25–1.25 nM (2–10 ng/ml) in blood plasma,

From the ‡Department of Biological Engineering, Massachusetts Institute of Technology, Cambridge, Massachusetts 02139; §Department of Pathology, University of Pittsburgh, Pittsburgh, Pennsylvania 15213

⌘ *Author's Choice*—Final version full access.

Received April 30, 2013, and in revised form, September 2, 2013

Published, MCP Papers in Press, September 9, 2013, DOI 10.1074/mcp.M113.030528

but as high as 25 μM in localized areas during wound healing (27, 28). Its ubiquitous presence, implication in cancer and vascular diseases, and use as a potential drug therapy have made PF-4 a key point of interest in influencing angiogenesis *in vivo* (27–30). In addition to inducing angiostasis, PF-4 can inhibit cell proliferation by halting S phase progression and reducing endothelial cell migration (25, 28, 30–32). Despite the wealth of information on PF-4 and its mechanistic effects on immune cells, scarce literature exists on the nature of the molecular signaling with endothelial cells to inhibit angiogenesis. Furthermore, the complexity of PF-4 mediated signaling and its potential to interact through multiple binding mechanisms makes it difficult to determine how PF-4 can interfere with angiogenesis (28, 29, 33, 34). Possible angiogenic signaling network interference mechanisms for PF-4 include the sequestration of growth factors and proteoglycans, antagonism of integrin-mediated signaling, or direct signaling through its chemokine receptor CXCR3, all of which have supporting evidence in previous literature (28). Along with the multiple mechanisms PF-4 may utilize for signaling, only limited studies on direct signaling elicited by PF-4 on endothelial cells have been reported; one of interest found that P38 MAPK can be activated via CXCR3 on endothelial cells cultured on plastic (35), whereas another, more definitive study showed PF-4 acting similarly to other CXCR3 ligands in activating PKA to prevent m-calpain-mediated rear de-adhesion of moving cells (36, 37). Furthermore, PF-4 could have variable sensitivities in different endothelial cell types because of heterogeneous expression of CXCR3 (38).

In our study, we sought to develop an approach to assess network-level signaling interactions between PF-4 and the major angiogenic inducer vascular endothelial growth factor (VEGF)[1] within a contextually relevant 3-D angiogenesis platform, in a controlled environment to understand what role these two factors may play. We developed methods to reduce extracellular matrix contamination in our samples and were able to successfully use a two-step lysis method with a MS compatible detergent-based lysis buffer. By taking advantage of iTRAQ-based multiplexed quantitation, we were able to collect quantitative phosphoprotein signaling data from our system with early and late temporal resolution. Using correlation network methods to observe differences in our system, we found that simultaneous treatment with PF-4 and VEGF induced changes in migrational pathway topology when compared with VEGF treatment alone. Most often, these changes appeared as losses in correlations between different migrational signaling proteins. We found that several different signaling pathways involved with migration were affected, including central proteins P38α MAPK, focal adhesion kinase (FAK), and Src family kinases. Furthermore, we found statistically significant differences in tyrosine phosphorylation when HDMVECs were stimulated with VEGF and PF-4, as opposed to only VEGF. In addition, we were able to recapitulate previously reported findings on how PF-4 infers its angiostatic effects on endothelial cells. Surprisingly, our data set revealed EphA2 receptor as a central node for PF-4 signaling, indicating that it may possess a complementary role in the balance of angiogenic and angiostatic effects.

To our knowledge, this is the first attempt at performing MS-based analysis of phosphotyrosine signaling networks within the context of an environment that is amenable to angiogenesis. Our work provides a step forward in applying high throughput and systems-level phosphoproteomics data collection to more physiologically relevant experimental conditions.

EXPERIMENTAL PROCEDURES

Cell Culture—Adult HDMVECs were purchased at passage five (Lonza, Walkersville, MD). Cells were cultured in EGM-2MV (Lonza) medium until near confluency. Once near confluency, cells were rinsed with 1× PBS (Invitrogen, Grand Island, NY) and detached by incubating with 0.05% Trypsin-EDTA (Invitrogen) for 3–5 min at 37 °C and 5% CO_2. Trypsin was neutralized by the addition of EBM-2 (Lonza) with 5% FBS (Thermo Fisher Scientific/Hyclone, Logan, UT) and 50 μg/ml gentamicin (Sigma-Aldrich, St. Louis, MO). Cells were pelleted at 450 × *g* for 5 min and resuspended in EGM-2MV before being seeded onto 50 μg/ml rat tail collagen I (BD Biosciences, Bedford, MA) coated tissue culture flasks at 5000 cells/cm^2. Medium was changed 24 h following seeding and replaced once every 48 h until nearing confluency. HDMVEC were grown up to passage 9 for use.

Collagen Gel Cultures—Collagen gels cultures were used to study capillary sprouting, as performed in a parallel study on HDMVEC migrational phenotype (22). Collagen gel solutions were made using 10× PBS (10%), collagen solution stock, and 1N NaOH (Sigma-Aldrich) added at 2.3% of the collagen stock solution volume used. Sterile MilliQ purified water was added to reach the desired total volume and kept on ice until use. One milliliter of collagen gel solution was added to each well in six-well plates (9.6 cm^2 per well). Gels were formed at a density of 2.0 mg/ml at approximately a pH of 7.2, and allowed to set at 37 °C for 2 h before being rinsed with 1× PBS. Gels were then preconditioned with EBM-2 with 5% FBS and 50 μg/ml

[1] The abbreviations used are: ANXNA1, Annexin A1; BCAR-1, Breast Cancer Anti-Estrogen Resistance 1; Cas1, CDK1, Cyclin Dependent Kinase 1; CTNND1, Catenin Delta 1 Isoform 1A (p120CAS); DYRK1B, Dual-Specificity Tyrosine-Phosphorylation Regulated Kinase 1B; DTT, Dithiothreitol; EBM, Endothelial Basal Media; EGM, Endothelial Growth Media; EphA2, Ephrin receptor EphA2; ephA1, Ephrin ligand A1; FAK, Focal Adhesion Kinase/Protein Tyrosine Kinase 2 (PTK2); FBS, Fetal Bovine Serum; HDMVEC, Human Dermal Microvascular Endothelial Cell; LC/MS/MS, Liquid chromatography tandem mass spectrometry; MAPK - Mitogen Activating Protein Kinase; Akt/PKB, Protein Kinase B; P38α, P38α MAPK/Mitogen-Activated Protein Kinase 14 ; PI3K, Phosphatidylinositide-3-kinase; PRP4K, Serine/Threonine Protein Kinase PRP4K; ErbB2IP, ErbB2 Interacting Protein; MPZL1, Myelin Protein Zero-Like 1; CD31, Platelet/Endothelial Cell Adhesion Molecule 1 (PECAM-1); IP, Immunoprecipitation; PBS-T, 0.1% Tween in 1X PBS; PF-4 - Platelet Factor 4; PKA, Protein Kinase A; PTPRα, Protein Tyrosine Phosphatase; Receptor Type Alpha; PTPRε, Protein Tyrosine Phosphatase; Receptor Type Epsilon; PXN, Paxillin; RTK, Receptor Tyrosine Kinase; SHC1, SHC transforming protein 1; SHP2, Protein Tyrosine Phosphatase; Non-receptor Type 11 (PTPN11); VEGF, Vascular Endothelial Growth Factor.

gentamicin for 2 days to minimize background changes and nonspecific ligand binding when dosing conditions were introduced to cells seeded on the gels.

HDMVEC were thawed and grown on 50 μg/ml collagen I coated tissue culture flasks up to passage 9, collected as above and counted using Neubauer-improved disposable C-Chip hemocytometers (INCYTO, Seoul, Korea) and seeded onto collagen gels at 50,000 cells/cm^2. Cells were allowed to adhere for 4–6 h at 37 °C in 5% CO_2 before rinsing with PBS and replacing the media with EBM-2 + 5% FBS and gentamicin. HDMVEC were allowed to incubate overnight. 24 h after seeding, plates of HDMVEC were dosed with 20 ng/ml VEGF-165 (Peprotech, Rocky Hill, NJ) and with or without 500 ng/ml PF-4 (Peprotech) across designated time intervals (0 min, 15 min, 30 min, 60 min, 6 h, 24 h, and 48 h). The concentration of PF-4 was selected based on results from previous work on HDMVEC (36, 37). In addition to significant dilution of precursor strength (see phosphotyrosine mass spectrometry and manual validation of mass spectral fragments in Supplemental Data), high error amplification, and previously reported dependence of the angiostatic behavior of PF-4 on the presence of angiogenic growth factors (28), the inclusion of a no VEGF (0 ng/ml) condition was omitted following initial testing.

Confocal Microscopy—Collagen gels were formed on 24 well glass bottom MatTek plates (MatTek Corporation, Ashland, MA) and HDMVEC were seeded following the protocol described above. Four hours after seeding, media were replaced with EGM-2MV + 20 ng/ml VEGF (40 ng/ml total). After 72 h, samples were fixed with 4% paraformaldehyde (Electron Microscopy Sciences, Hatfield, PA) for 30 min and rinsed gently with PBS before being permeabilized with 0.1% Triton-X (Sigma-Aldrich) in PBS. The fixed samples were incubated with 1:100 Alexa 568-conjugated phalloidin (Invitrogen) for actin filaments and 1:200 rabbit polyclonal anti-vascular endothelial cadherin (VE-cadherin) antibody (Enzo Life Sciences, Farmingdale, NY) in 1× PBS with 0.5% BSA for 1 h before being rinsed with PBS. Samples were then stained with 1:1000 DAPI (Invitrogen) and imaged on an Olympus FV1000 Multiphoton Laser Scanning Confocal Microscope using Imaris 7.0.0 (Bitplane, South Windsor, CT).

Microfluidic Migration Assay Platform—These follow protocols as described previously (22, 39). For more information, please refer to Supplemental Data and Methods.

Detergent Surface Lysis With Subsequent Urea Lysis—Detergent-based lysis buffer was made following previously established protocols (40). Slight modifications were made to the base protocol to maintain compatibility with MS lysate preparation protocols. Cell lysis buffer consisted of 1% Triton X-100, 50 mM β-glycerophosphate, 10 mM sodium pyrophosphate, 30 mM sodium fluoride (Sigma-Aldrich), 50 mM Tris (Roche Applied Science, Indianapolis, IN), 150 mM sodium chloride, 2 mM EGTA, 1% Protease Inhibitor Mixture (Sigma-Aldrich) and 1% Phosphatase Inhibitor Mixture Sets I and II (EMD Calbiochem, Gibbstown, NJ). Following a rinse with cold PBS with the plates on ice, 200 μl of cold lysis buffer were gently added to the top of each gel. Plates were then quickly transferred to a Model 1000 standard orbital shaker (VWR International, Radnor, PA) set at ~185 rpm for 15 min at 4 °C. Following lysis, lysate from each well of a six-well plate was consolidated into one sample, defined as a biological replicate in our analysis at ~1.2 ml volume and mixed with 3.6 ml of 8 M urea with 1 mM activated sodium orthovanadate (Sigma-Aldrich) to a final urea concentration of 6 M. Samples were then immediately snap frozen in liquid nitrogen before placing into storage at −80 °C.

Western Blotting—Signaling in HDMVEC seeded on collagen gels was assessed under the dosing conditions indicated above. Samples were then lysed using the detergent-based lysis buffer described above for MS sample preparation. In addition to the components listed above, 1 mM DTT and 1 mM PMSF were included to prevent phosphatase activity and protein degradation (40). Six-well plates were placed on ice and rinsed with cold PBS before the addition of 200 μl of lysis buffer to each well. Cell scrapers were used to break up the collagen gel and facilitate lysis of cells. Samples were collected and spun down in an ultracentrifuge at 14,000 rpm (~16,000 *g*) for 12–15 min until debris was pelleted from the supernatant. The NuPage Novex System (Invitrogen) was used to run gel electrophoresis, where lysates were loaded with 6× reducing buffer (Boston BioProducts, Worcester, MA) in 4–12% Bis-Tris gels (Invitrogen) and transferred to polyvinylidene fluoride membranes (Bio-Rad, Hercules, CA). Membranes were blocked with 5% BSA in 0.1% Tween in PBS (PBS-T) and incubated with antibodies for β-actin (1:5000), α/β tubulin (1:5000), phospho-ERK1/2 (1:5000), phosphoY772-EphA2 (Tyr772) (1:1000) (Cell Signaling Technology, Beverly, MA), and EphA2 (1:1000) (Cell Applications, San Diego, CA) overnight at 4 °C. Membranes were washed and then incubated for 1 h with horseradish peroxidase-conjugated antimouse and/or antirabbit antibodies (Amersham Biosciences/GE Healthcare Biosciences, Pittsburgh, PA) at 1:10,000 dilution in PBS-T with 5% blotting grade nonfat dry milk (Bio-Rad). Membranes were subsequently visualized using chemiluminescent ECL kits (Amersham Biosciences/GE Healthcare Biosciences) on a Kodak Image Station (Perkin Elmer, Waltham, MA).

Phosphotyrosine Mass Spectrometry—Sample processing followed protocols for chemical reduction, alkylation, trypsin digestion, and fractionation as previously described (41, 42). Briefly, groups of eight samples were labeled with eight unique isobaric iTRAQ reagents (AB SCIEX, Framingham, MA) for 2 h at room temperature. Following labeling, samples were combined and concentrated before immunoprecipitation (IP) with a mixture of antiphosphotyrosine antibodies (4G10 (Millipore, Billerica, MA), pTyr100 (Cell Signaling), and PT-66 (Sigma), 12 μg of each) immobilized onto protein G agarose beads (Calbiochem) in iTRAQ IP buffer (100 mM Tris, 100 mM NaCl, 0.3% Nonidet P-40, ph 7.4) (Sigma-Aldrich) overnight at 4 °C. Beads were washed four times in rinse buffer (IP buffer without Nonidet P-40) and phosphotyrosine-containing peptides were eluted with glycine buffer (100 mM, pH = 2) at room temperature for 30 min on a rotator. Phosphopeptides were further enriched by immobilized metal affinity chromatography (IMAC) on a custom-packed 200 μm × 10 cm column with Poros MC 20 μm beads (Invitrogen). Phosphopeptides were eluted with phosphate buffer (250 mM, pH 8.0) directly onto a custom 100 μm x 10 cm precolumn packed with 10 μm YMC-Gel ODS-A beads (Waters Corporation, Milford, MA). The precolumn was immediately washed and brought in line with a custom 50 μm × 10 cm analytical column packed with 5 μm YMC-Gel ODS-AQ beads with 120 angstrom pores (Waters Corporation), and with an integrated sub-μm nanospray tip pulled with a laser puller (Sutter, Novato, CA). Each tip was examined by microscopy with a calibrated objective and tested extensively with single femtomolar quantities of peptide standards before use. Analysis and quantification of eluted peptides were conducted on an Orbitrap Elite mass spectrometer via nano-ESI LC/MS/MS (Thermo Fisher Scientific) with a tandem MS top ten data-dependent acquisition method. Peptides were eluted with a binary gradient with an aqueous solvent of 0.2 M acetic acid in ultrapure water and an organic solvent of 0.2 M acetic acid in 90% acetonitrile and 10% ultrapure water. The gradient was 0–13% organic from 0 to 10 min, 13% to 42% from 10 to 105 min, 42% to 60% from 105 to 115 min, 60% to 100% from 115 to 120 min, held at 100% organic from 120 to 128 min, and washed indefinitely with aqueous solvent until peptides stopped eluting. The flow rate was initially set at 20 nL/min and then dropped to 5–10 nL/min once peptides began eluting.

Raw files were processed with MSQuant v2.0b7 software and DTASupercharge (43), followed by peptide sequence and protein identification with Mascot v2.1.03 (Matrix Science, Boston, MA) (44).

Mascot searches were run in MS/MS ion search mode with the following parameters. Fixed modifications included iTRAQ8plex (K, N-term), and Carbamidomethyl (C), whereas variable modifications were Oxidation (M), Phospho Serine/Threonine (ST), and Phospho Tyrosine (Y). Monoisotopic mass values were selected with no restrictions on protein mass. A tolerance of 10 ppm was selected for peptide mass and 0.8 Da for fragment mass tolerance, with a maximum of two missed trypsin cleavages permitted. The instrument type was specified as an LTQ-Oribitrap. Because the culture system of HDMVECs was human in origin, the database was limited to the 2009 NCBI human proteome database in all searches (*H. sapiens*), with 37,743 total entries. The top 1000 peptide hits were reported, neglecting protein significance score cutoffs, because of the extensive phosphotyrosine enrichment performed. Because of the challenges associated with using a collagen gel culture system, an initial MASCOT peptide score threshold of 20 was implemented before initial data processing and normalization to protein supernatant values. In the cases of multiple matches, the query with the highest score and smallest expect value from Mascot was selected. For search results file outputs (both phosphotyrosine enriched immunoprecipitates and IP supernatants), please see Supplemental Data. All mass spectrometry proteomics data were deposited to the ProteomXchange Consortium (http://proteomecentral.proteomexchange.org) via the PRIDE partner repository with dataset identifier PXD000462 (114).

Manual Validation of Mass Spectra Fragments—Because our work involved specific phosphorylation of amino acid residues, each tyrosine phosphorylation site was subjected to manual validation. Phosphopeptide scores and signals were thresholded for significant hits (score >20) and values were normalized to a master lysate (50 ng/ml VEGF treatment for 15 min) and normalized to total protein values obtained from an LC/MS/MS analysis of iTRAQ channel intensities of the IP supernatant. Initial methods to normalize to a master control condition with no stimulation (no VEGF) yielded a response with high noise to signal amplification because of the absence or minimal signal present in this condition. Each nonzero normalized mass spectra output (where iTRAQ for at least 5 of 8 tags were nonzero) was manually validated by hand following previously described guidelines to ensure correct sequence identification and phosphosite assignment (45). Peaks were compared with theoretical values for each of the peptides assigned by Mascot using the MS-Product component of Protein Prospector v5.10.9 (Baker, P.R. and Clauser, K.R. http://prospector.ucsf.edu). The processed, validated mass spectra data are also included in the Supplemental Data, as well as scans that were rejected because of precursor contamination, as indicated in the added header on each scan plot. Amino acid residue locations of phosphorylations on peptides were verified using PTMScout (46) in addition to the aforementioned manual validation.

Data Processing and Statistical Analysis—Data from three biological replicates (with two technical replicates per biological sample) were consolidated into one data set for assessing phosphoprotein levels. To quantify across the six mass spectrometry analyses, a master lysate sample included in each batch of samples processed for mass spectrometry was used as a normalization factor to compare across several runs. Statistical analysis of time course data was performed using Student's *t* test (Microsoft Excel). Methods to quantify signaling node relatedness using correlation network modeling follow those previously described (47). At every time point, geometric means of the phosphorylation fold change relative to a master lysate were calculated for each protein that had at least two nonzero measurements across two biological replicates (two technical replicates each). For time points and proteins where only one measurable MS value was collected and identified from the total pool of replicates performed, the single replicate value was used as a measure of best estimate of phosphorylation.

Of the resulting MS data, 37 phosphosites fulfilled the full time course criterion for initial modeling setup. Pearson correlation coefficients were calculated between each pair of phosphosites using the 37×6 data matrix. Statistical significance of pairwise correlation coefficients was assessed using the permutation test by shuffling time course data ($n = 100{,}000$). The overall data set provided $37 \times 36/2 = 666$ unique pairwise correlation coefficients and p values (self-correlations ignored).

RESULTS

Optimization of Collagen Gel Culture System for Collection of Phosphoprotein Signaling Data—HDMVEC seeded on collagen gels had the capability to undergo sprouting (Fig. 1, Video S1). Although the occurrence of sprouting events are generally uncommon *in vivo* (as only a few cells eventually break away from the bulk), the collagen gel culture system provided us with both a system that could provide quantitative intracellular signaling analysis and the future potential to capture extracellular endothelial response behaviors associated with angiogenesis. However, conventional methods of harvesting cell lysates provided either insufficient total protein, large volumes of diluted samples, or excess collagen. Multiple alternative methods were evaluated for maximizing cell lysate retention for efficacious processing. These included: (1) centrifugation of urea-lysed samples with collagen gels; (2) urea-lysis, freezing, thawing, and centrifugation of samples; (3) urea-lysis and syringe filtration of lysate using 0.22 μm filter; (4) initial cell detachment using collagenase cocktails followed by urea lysis; (5) urea lysis followed by IP incubation with collagen antibodies; (6) centrifugation of detergent-lysed cells followed by acetone precipitation and resuspension in urea lysis buffer; and (7) surface lysis of HDMVECs followed by suspension in urea buffer. Lysis procedures of samples grown on collagen gels were assessed by visualizing phospho- and total ERK1 and 2 levels, and surface lysis protocols were found to provide the best results. The assessment validated our ability to detect phosphoproteins using surface lysing protocols, thereby indicating that we could potentially detect phosphorylation sites with the use of the collagen gel system with mass spectrometry methods (see Supplemental Data, Fig. S1). In addition, other phospho-peptides (P38, Akt, PKA) were also evaluated during the validation process (data not shown).

Time-resolved Tyrosine Phosphorylation Measures by Quantitative Mass Spectrometry Indicate Statistically Significant Differences over the Course of Stimulation—Following manual validation of spectra outputs, 133 phosphorylation sites across 92 proteins were observed in our data set. Out of the 92 unique proteins identified, 33 proteins identified had at least one measurable scan for more than one condition (37 phosphosites overall). Of these 33 proteins, we observed 22 proteins that had statistical data available at all time points tested for both treatment conditions (26 total phosphosites

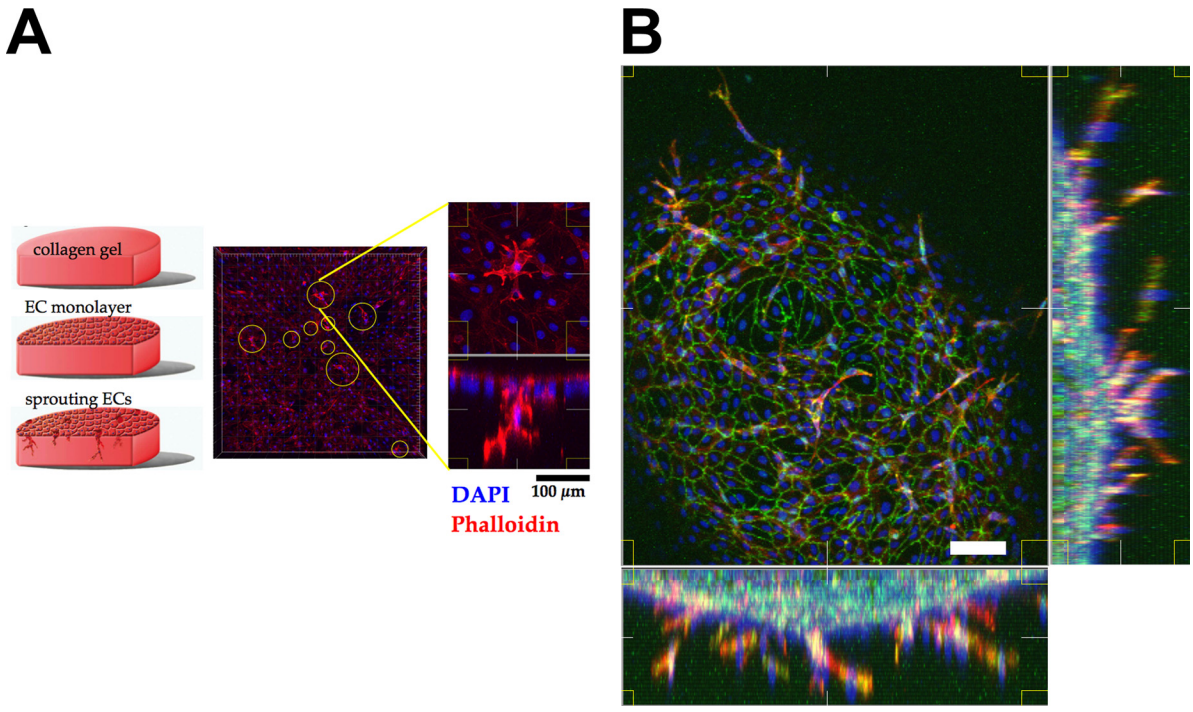

FIG. 1. **Collagen gel culture enables signaling analysis of endothelial sprout initiation.** Sprouting events could be observed within 24 h after HDMVEC seeding on collagen gels. Actin filaments were stained with phalloidin (red) and cell nuclei were stained with DAPI (blue) and VE-Cadherin (green). A general schematic of the collagen gel set-up is shown with multiple sprouts observed in the yellow circles 18 h after seeding (*A*). A higher magnification and its respective Z projection of an initiated sprout into the collagen are shown for a selected sprout. Orthogonal Z projections of an HDMVEC culture into a collagen gel are shown after 72 h (*B*), with significant invasion into the collagen gel. The gel cultures are more physiologically representative of the environment that endothelial cells observe *in vivo*, as opposed to strictly culturing on tissue culture plastic which do not allow angiogenic behavior to be simulated or observed. Using this culture system, we were able to observe angiogenic sprouting as well as signal transduction pathways relevant to the process. Scale bars = 100 μm.

with statistical data), where 17 of the proteins had statistically significant differences following the addition of PF-4. The temporal signaling dynamics for these proteins are shown in Fig. 2, with the statistical significance marked by their respective levels. These data were interpreted as a comparison between VEGF only and VEGF cotreatment with PF-4 as crosstalk pathway activation because of the presence of PF-4. A third treatment condition with PF-4 by itself in absence of VEGF did not exhibit any large, statistically significant effects on phosphorylation compared with the control condition (data not shown), and hence comparisons were made with VEGF present in both conditions. The condition of no stimuli (no VEGF, no PF-4) was not included because of initial analysis yielding little or no signal present. The lack of significant differences for PF-4 only treatments does not necessarily rule out the importance of independent signaling by PF-4. Most likely, the preponderance of PF-4's impact on signaling occurs in conjunction with angiogenic signaling processes as a potential modulatory influence.

There was a persistently higher level of Annexin A2 phosphorylation for the majority of the time course when PF-4 was present, which became lower at later time points. On the other hand, Annexin A1 experienced an early attenuation of signal intensity at 15 min when PF-4 was present, although signaling became indistinct from conditions where PF-4 was absent. Cell cycle regulating protein cyclin dependent kinase 1 (Cdk1) appeared to have an initial decrease in signal followed by a delayed response in activation when PF-4 was present. For Ephrin A2 receptor (EphA2), whereas a stark drop in signal occurred at 30 min when HDMVEC were dosed with VEGF, PF-4 treatments experienced an increase in signaling. Similarly, Src family kinases Fyn and Lyn experienced an increase of phosphorylation in early time points when both PF-4 and VEGF were present. Interestingly, both experienced a sharp decline during signaling around 60 min compared with VEGF treatment only. On the other hand, FAK appeared to have an attenuated phosphorylation signal at 60 min before being much more actively phosphorylated at later time points. Dual phosphorylation of P38α at T180 and Y182 decreased at 15 min in the presence of PF-4, although relative phosphorylation levels of Y182 increased at 30 min. Paxillin and CD31 both had higher phosphorylation expression levels when PF-4 was present relative to VEGF treatment by itself, indicating that they may be positive signaling mechanisms employed by PF-4, although there was no statistical significance observed between the two conditions ($p > 0.05$).

Many of the other proteins shown in Fig. 2 had complex signaling which were difficult to interpret because of lack of

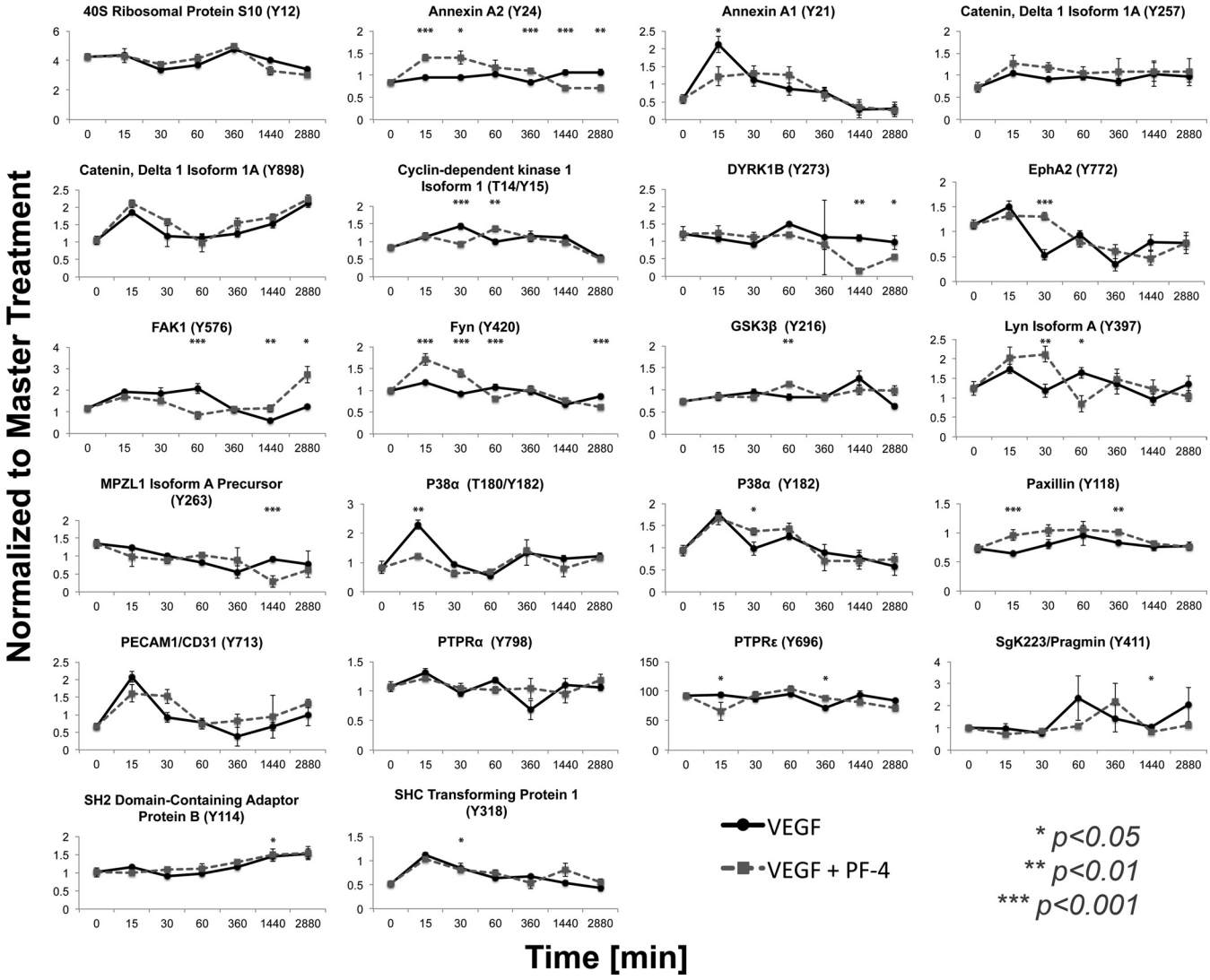

FIG. 2. **Signaling dynamics from time resolved tyrosine phosphorylation measurements by quantitative mass spectrometry.** Of the 133 manually curated phosphorylation sites, only 37 had a full time course data set, with 22 phosphosites having at least two readings per time point in both treatment conditions. The phosphorylation level of these sites is provided for two different treatment conditions: 20 ng/ml VEGF (VEGF), and 20 ng/ml VEGF + 500 ng/ml PF-4 (VEGF + PF-4). Raw signal measurements were normalized to total protein values and reported as relative proportions to a master lysate stimulated with saturating 50 ng/ml VEGF. Notable temporal increases in signaling dynamics following PF-4 cotreatment were observed for Annexin A2(Y24), EphA2(Y772), Fyn(Y420), GSK3β (Y216), Lyn(Y397), P38α(Y182), Paxillin(Y118), and SHC1(Y318). Attenuations in signaling were noticed for Annexin I(Y21), DYRK1B(Y273), and focal adhesion kinase FAKY576) with PF-4 present. Changes were not mutually exclusive in the same time course data as both increases and decreases in phosphoprotein levels were observed at different time points for many of these proteins as well as Cdk1(T14/Y15) and MPZL1(Y263). Treatment with PF-4 alone yielded noninformative results. Statistical analyses performed using Student's *t* test found a majority of statistically significant differences to occur in early time points (first 60 min), indicating that early signaling most likely informs endothelial response. Errors bars represent standard error. Statistical significance indicated by asterisks: * for $p < 0.05$, ** $p < 0.01$, and *** $p < 0.001$.

statistical significance ($p < 0.05$) and/or very minor difference in phosphorylation between the two treatment conditions. Although statistical significance was found to occur at various points in time for the different signaling proteins in the data set, the majority of these significant differences occurred at early time points within the first hour of dosing, indicating that most of the phenotypic responses mediated by these two signaling molecules were dictated by early exposure to these cytokines rather than later signaling. These complex signaling dynamics include receptor protein tyrosine phosphatases PTPRα and PTPRε, CD31, pragmin, and cdk1. In fact, observing the behavior of cdk1 across time appears counterintuitive as well; rather than expecting PF-4 to inhibit mitosis as observed in previous findings (32), the presence of PF-4 actually reduces the phosphorylation levels at 30 min relative to the sole treatment with VEGF. However, a caveat of the previous findings were from cells cultured on coated plastic, which may have inherent differences from the environmental

TABLE I

Important phosphorylation sites involved with PF-4 and VEGF crosstalk and their previously reported functions. A subset of the phosphorylation sites found to be involved with PF-4 and VEGF signaling in the sprouting angiogenesis data set is highlighted in this table, including 22 of the 37 phosphoproteins that were found to have complete coverage across all time points in the data set. Previously reported functions for these proteins and phosphorylations are shown from different cell systems, as well as some that have been reported to play roles in angiogenesis. Although they may have been reported to have roles in other cell phenotypes, there may be overlap with the PF-4 and VEGF signaling system, such as the potential importance of cell migration and polarization in orchestrating blood vessel formation

Protein name (and Aliases)	Phosphorylation(s)	Reported functions	References
ANXNA1	Y21	EGFR binding, inward vesiculation	(90, 91)
Cas1 (BCAR-1,Crk1)	Y234, Y387, Y410	Migration, invasion, differentiation	(65, 66)
CTNND1 (p120CAS)	Y257, Y898	Uncharacterized	(92, 93)
CDK1	T14/Y15	G1 arrest	(94–98)
DYRK1B	Y273	Catalytic domain autophosphorylation	(99)
EphA2	Y575, Y772	Activation loop	(100, 101)
Erbin (ErbB2IP)	Y1104	Uncharacterized	(102)
P38α	T180/Y182	Kinase activation	(59–61)
MPZL1	Y263	SHP2 docking	(103)
PXN	Y118	Cell polarization and motility	(104, 105)
CD31	Y713	Src/SHP2 binding site	(68–71)
SHP2	Y62	Uncharacterized	(106, 107)
PTPRα	Y798	Grb2 docking	(108, 109)
PTPRϵ	Y696	Uncharacterized	
Fyn	Y420	Activation	(110)
FAK	Y576	Activation	(64, 111)
PRP4K	Y849	Uncharacterized	
SHC1	Y318	Ras activation, adaptor protein	(112)
Lyn	Y397, Y508	Enzymatic activation (Y397) and inhibition (Y508)	(113)

context applied here. Although there is a delayed increase in Thr14/Tyr15 phosphorylation at 60 min, simultaneous treatment with PF-4 maintain a slightly lower level of this inhibitory phosphorylation.

Significant Phosphoprotein Sites That are Detected Are Strongly Associated With Influencing Cell Migration Pathways—Following manual validation of the tandem mass spectra, the remaining phosphosites in the curated data were evaluated using reports in previous literature to determine their potential roles here in inflammatory angiogenesis pathways. These functions are reported in the table, along with their sources and alternative names (Table I). Most of the phosphosites are known to be involved in cell polarization and migration activity, including phosphosites on FAK, Src family kinases, Cas1, and Paxillin. Although the functional association of these sites were determined in cell lines, they are known to perform similar or identical functions across many different cell types as well as across species that have homologous proteins; it is therefore likely that these functions are recapitulated in this context.

Correlation Network Modeling Reveals Significant Changes in Protein Interactions Involved in Inhibiting Cell Migration Mechanisms—With a relatively large data set, it is difficult to infer the exact mechanisms by which the introduction of PF-4 changes the overall signaling landscape in HDMVEC angiogenesis. To make sense of the time course data, a network correlation model was employed to evaluate the topology changes in signaling pathways between the two treatment conditions. Pearson's pairwise linear correlation coefficients were evaluated and compared for differences between the two conditions, with the strength of the correlations shown as a heatmap (Fig. 3). A considerable number of proteins in the data set did not possess more than one replicate at each time point for the two conditions tested. To expand our analysis beyond the 22 phosphosites and provide a wider breadth of coverage, we used the single replicate as a representation of the signaling intensities to increase our analysis to include 37 phosphosites. Overall, there appeared to be many negative, or low correlations present in the data set, particularly with proteins associated with BCAR-1 (Cas1) such as FAK, P38alpha, Fyn, and protein tyrosine phosphatases (Fig. 3*A*). On the introduction of PF-4, many of these correlations are reversed; in fact, there are a greater number of strong, positive correlations when VEGF and PF-4 are co-treated (Fig. 3*B*).

For example, although ErbB2IP/Erbin was positively correlated with almost all proteins except BCAR-1/Cas1, GSK3β, Paxillin, Pragmin, TIE1, Tyk2, and SHB in VEGF treatments, these positive correlations all became inversely correlated or reduced in strength following co-treatment with PF-4. In addition, Shp2, PLCγ, MPZL1, and P38α are new, strongly negative correlations with Erbin following PF-4 treatment. These inversions in correlation trends were similarly observed for most of phospho-Y575 EphA2 and FAK interactions (Fig. 3*B*). Likewise, many other proteins had the opposite trends in correlations occur, including many of the associations with phospho-Y257 Catenin δ1 and Src family kinase Fyn (Fig. 3).

To reduce the number of observations made, as well as to extract the most accurate and significant data from signaling

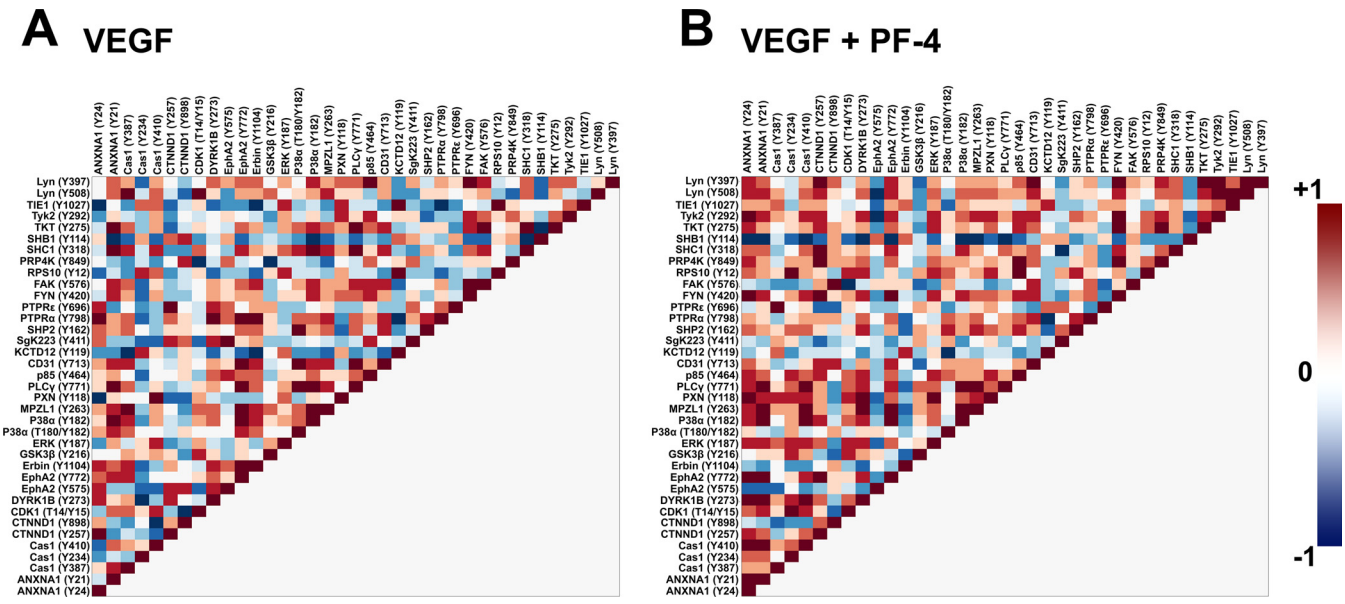

FIG. 3. **Heatmap of pairwise correlations in both VEGF with and without PF-4 treatments.** Linear Pearson pairwise correlations for VEGF with and without PF-4 were calculated for the phosphorylation fold changes measured for each time course. There are distinctive shifts in the distribution of correlations between VEGF (*A*) and VEGF+PF-4 (*B*) treatments, particularly with the higher number of negative correlations present when PF-4 is absent. Phosphorylation changes were represented by the ratio of geometric means to a master control to reduce potential effects of outliers in the population distribution.

dynamics, correlation values obtained for the full data sets were compared with a distribution of expected values generated from randomizing the original data set 100,000 times. This approach provided an estimate of the statistical significance of each correlation (*p* values), of which we considered those that appeared with $p < 0.05$ as significant. Although there were relatively fewer overlaps of correlational changes, the most interesting observation of the changes in correlation coefficients were those following PF-4 treatment. Of the most significant correlations ($p < 0.05$) that we observed in our system, there were only 65 correlations in the VEGF treatment compared with 79 correlations that were significant following co-treatment with PF-4 (Fig. 4). Of the total 144 unique correlations between the two conditions, 18 are shared between the two; 47 correlations are present only when VEGF is present and disappear following PF-4 addition; 61 correlations are present only when the two cytokines are simultaneously present. Interestingly, these correlations with $p < 0.05$ were all strong, positive correlations; no negative correlations were observed. An increase of signaling correlations following the addition of PF-4 may be indicative of synergistic pathway activations.

For a more intuitive understanding of the correlations with $p < 0.05$, signaling diagrams were plotted to assist in data interpretation, where non-directional edges were representative of pairwise correlations (Fig. 5). The topologies of interconnected correlations are shown in the flow chart where red edges indicate correlations present in VEGF, and green edges indicate correlations present in VEGF+PF-4. Roughly, the topographical interpretation could be that the red edges are lost or "inhibited," whereas green edges are activated following PF-4 treatment. From our correlation network analysis of signaling topology changes, we observed that a significant number of correlations appeared centering around EphA2 when PF-4 was present. It appeared that EphA2 phosphorylation was strongly correlated with Src family kinases, P38α MAPK, Shc1, DYRK1B, Catenin δ1, and Annexin A1, a majority of which have been previously associated with regulating cell polarization and migration. On the other hand, many correlations that were present in VEGF treatment involving FAK disappeared following PF-4 addition. Likewise, loss of correlations also occurred centering around CD31, including correlations with EphA2, Shp2, receptor protein tyrosine phosphatases.

With a focused subset of proteins such as ours, it is difficult to generate a relevant model of pathways, but even a sparse model characterizing relational associations can provide some insights about how these proteins might influence activities via pathway crosstalk. Our correlation network model demonstrated CD31, P38α, Fyn, and EphA2 to be central nodes in both signaling environments to the changes in protein correlations following PF-4 treatment. Although PF-4 attenuated many of the signals observed following VEGF treatment, the signals that increased in correlation strength were of particular interest. In fact, our significant correlations with $p < 0.05$ indicate positive correlations of multiple signaling events; no negative correlations were found. Coupling the presence of P38α, Fyn, and EphA2 as central nodes with the time course data collected (Fig. 2) suggests that VEGF with

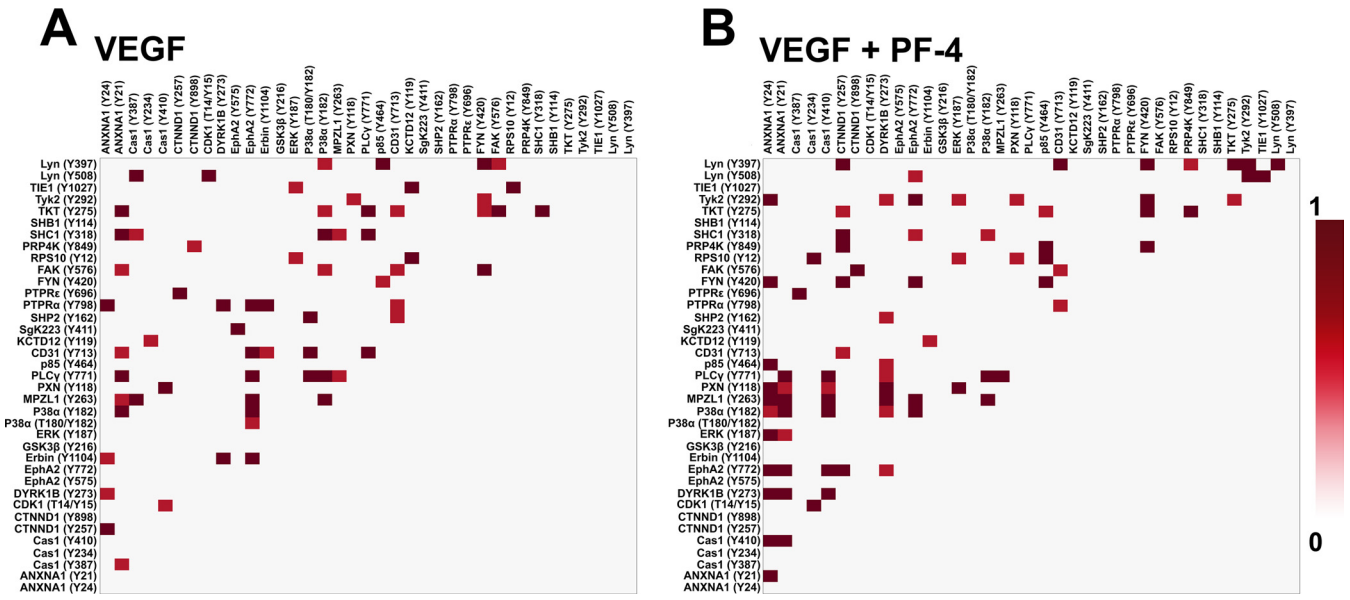

FIG. 4. **Heatmaps of significant pairwise correlations in VEGF and VEGF + PF-4 treatments.** Following significance evaluation with permutation tests, the majority of the pairwise correlations that remained are shown in the heatmaps above for VEGF (*A*) and VEGF + PF-4 (*B*), filtered for pairwise correlations that have $p < 0.05$. Only positive correlations remain in either condition indicating that signaling in both treatment conditions occurs cooperatively and not antagonistically with other proteins.

PF-4 tends to generally increase phosphorylation levels while they decrease over time in VEGF only conditions.

Increased Phosphorylation and Total Protein Levels of EphA2 are Indicated to Mediate PF-4 Signaling Effects—As a follow-up of our analysis to validate the changes observed for EphA2, Western blots on phosphorylated tyrosine 772 and total EphA2 (Fig. 6) were performed. Seven replicates were performed of the total and phospho-EphA2; a representative Western shown in Fig. 6*A*. Both total and phosphorylated EphA2 levels increased in HDMVECs that were treated with PF-4 and VEGF as opposed to VEGF by itself. A semiquantitative assessment of these concentrations was performed using pixel intensity data of the Western blots. The mean values and their standard errors were calculated from the seven Westerns performed (Fig. 6*B*). There was an increase in both phospho-Y772 and total EphA2 following the addition of PF-4 at 30 min compared with VEGF by itself. Previous work has found that binding of soluble ephA1 ligand to EphA2 can initiate rapid activation and degradation of the total receptor expression on cells, which PF-4 treatment may modulate (48–50). Although no statistical significance was observed for phospho-Y772 EphA2, statistical significance was found for total EphA2 ($p < 0.05$ by nonparametric statistical test Wilcoxon rank sum) between the two treatment conditions. Phosphorylation of tyrosine 594 and serine 897, sites known to be responsible for kinase activity regulation of EphA2 following Y772 phosphorylation, were difficult to observe in our system, most likely because of rapid dephosphorylation by phosphatases and negative feedback loop interactions (51–53). These phosphorylations were not detected in our MS or Western blot samples (data not shown).

Attempts to finely tune total and phospho-EphA2 concentrations are difficult in primary HDMVECs, as phosphoinhibitors, such as epigallicotechin gallate or lithocholic acid, were difficult to use to inhibit EphA2 because of their nonspecific effects on other multiple proteins (54, 55). Additionally, attempts to reduce both phospho-EphA2 and total EphA2 concentrations using siRNA reduced cell retention because of the requirement of EphA2 for cell-cell interaction and substrate adhesion (Supplemental Data, Fig. S2).

DISCUSSION

With the advent of new systems-level phosphoproteomic analysis methods, there is an increasing ability for large data sets to be collected. In many cases, a more thorough survey of the quantitative signaling in a system can be completed (56). Unfortunately, the caveat to these large data sets are that many of these phosphosites and protein targets are still not completely characterized, leaving many of the possible roles and functions as potential mysteries. Inflammation is a very complex process convoluted by multiple factors and events. In our system, we sought to use MS-based methods to shed further light on how angiogenesis might occur in the inflammatory environment, when exposed to strong early positive and negative regulating factors of angiogenesis.

Although there indeed were statistically significant differences at later time points (24–48 h) between VEGF with and without PF-4 conditions, we observed the majority of these differences to occur early in signaling, within the first 60 min of treatment with the signaling factors. It appears that early signaling mechanisms that are initiated by the two cytokines influence the response behaviors observed long after. Past

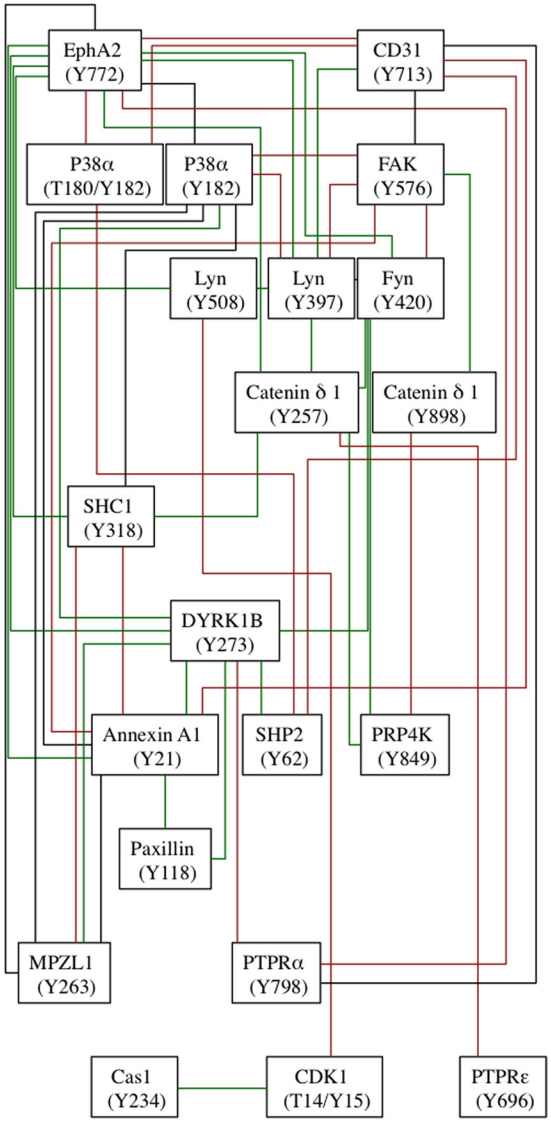

FIG. 5. **Correlative network connections between significant phosphosites involved with the VEGF and PF-4 signaling.** Significant pairwise correlations from above ($p < 0.05$) were compared between the two treatment conditions where HDMVECs were dosed by VEGF alone or in conjunction with PF-4. To identify potential dynamic changes in the topography of signaling, the presence or absence of correlations between the two conditions were mapped out. Black edges represent strong positive correlations present in both the presence and absence of PF-4 co-treatments with VEGF. Red edges indicate correlations present when endothelial cells were dosed with VEGF only. Green edges indicate correlations that appeared only when HDMVECs were simultaneously treated with PF-4 and VEGF and not with VEGF only. There were a larger number of correlations that appeared only with VEGF treatment, such as those centered around CD31 via shear stress response as well as migratory-centric pathways involving FAK and Src Family Kinases. As expected by many of the reported angiostatic effects of PF-4, red edge correlations (VEGF only) disappeared for FAK and other migratory pathways. Interestingly, many new green edge correlations (VEGF + PF-4) appeared around EphA2, contrary to its previously reported roles in promoting angiogenesis.

studies have found that early signaling pathway activation informs cellular response long after the signaling pathway actions have dissipated (57).

Similar to previous findings, we found that P38α MAPK activity increased following PF-4 dosing (35). P38α MAPK activity has been found to suppress endothelial cell migration capacity and may have similar anti-migratory effects in our system (58). This finding potentially agrees with previous data on PF-4 signaling through P38α to exert its angiostatic activity, despite the considerable differences in experimental approaches (35). Although we used HDMVEC cultured on gels (providing sprouting potential), the previous studies have focused primarily on cultured microvascular endothelial cells directly on tissue culture plastic, thereby providing the possibility that signaling dynamics may differ because of the environments used. However, we did observe a decrease in T180 phosphorylation because of PF-4's presence at 15 min, which has been previously reported to be important in kinase activation. This decrease in threonine phosphorylation can affect the overall efficacy of the kinase's activity; as kinase activity is strongly dependent on the presence of both phosphorylation sites, particularly that of T180 (59–61).

We observed an initial decrease followed by an increase in later times for FAK signaling when PF-4 was simultaneously present with VEGF. Phosphorylation levels dipped below that of VEGF at 60 min, before increasing at later time points to levels higher than with VEGF alone. These phosphoprotein level changes and protein interactions may reflect PF-4's regulatory influence on reducing endothelial migration, which agree with previously found data (25, 30). The modulations in Fyn and Lyn also lend credence to PF-4 influencing VEGF mediated signaling. Although Fyn has been found to inhibit cell migration following VEGF stimulation, Lyn promotes it as a positive regulator (62). Both show increased signaling when PF-4 is introduced, albeit Lyn has decreased signaling at 60 min, possibly contributing to PF-4's ability to inhibit cell migration. FAK promotes angiogenesis and cell migration in a Src-dependent manner in which PF-4 may interfere (63). The notion that PF-4 is interfering with angiogenesis via Src family kinases is also supported by the phosphorylation levels we observe for Tyr576 on FAK, as it is a result of being in proximity to Src family kinases, such as Fyn and Lyn (64). Cas1 has been reported in previous literature to be important in the regulation of cancer cells (65, 66), as well as dynamic regulation of cytoskeletal components in conjunction with FAK (67). The temporal observations and correlation topography involved with PF-4 agree with previously reported findings on PF-4 exerting its effects primarily by affecting cell migration pathways.

In addition to the migratory pathways we observed being modulated by PF-4, CD31 phosphorylation appeared to be important in VEGF conditions, which disappeared when treatment with PF-4 was applied. Phosphorylation of Y713 on CD31 has been implicated to be a result of endothelial cell

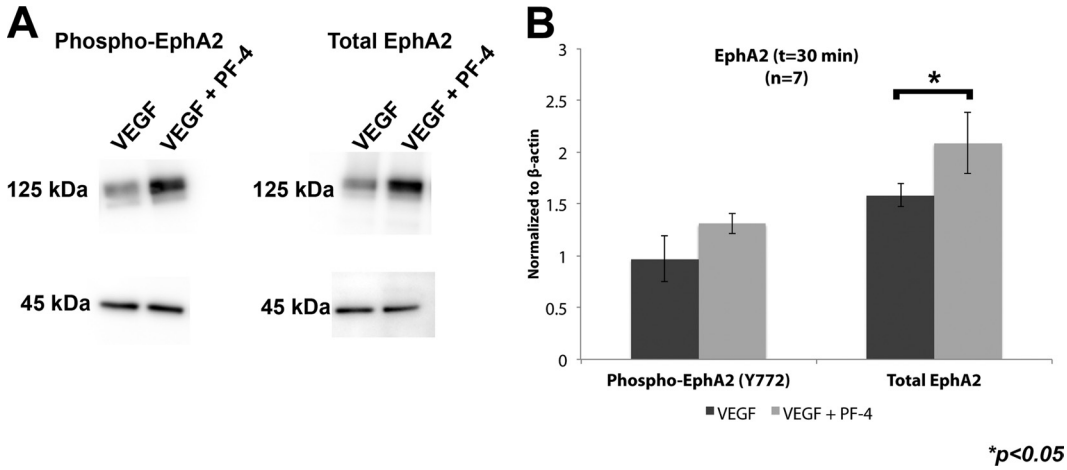

FIG. 6. **Western blots of phosphorylated and total EphA2 indicate increases in both following co-treatment of HDMVECs with PF-4 at 30 min.** Representative Westerns (*A*) are shown for both phospho- and total EphA2. Semiquantitative analysis of Western blots using pixel intensity data ($n = 7$) yielded increases in both total and phospho-EphA2 when PF-4 was added (*B*). The phospho-EphA2 increase agrees with the signaling data obtained using mass spectrometry. These data indicate the potential role that EphA2 may play in mediating the signaling crosstalk effects by EphA2. Although there was no statistical significance found in phosphorylation levels between VEGF and VEGF with PF-4 treatment, statistical significance was found for total EphA2 levels between the two treatment conditions ($p < 0.05$, Wilcoxon rank sum test). Error bars represent standard error.

response to shear flow, and is responsible for mediating T-cell migration to inflamed environments (68–71). With the correlation topography we observe, it appears that phospho-Y713 on CD31 may also be connected to the Src family kinases and can influence cell migration pathways via this mechanism (72). There is additional evidence of the possible influence of CD31 phosphorylation on migration behavior because of loss of correlations with Cas1, SHC1, and Annexin A1.

In the context of angiogenesis, Annexin A1 has been reported to have both angiogenic and anti-inflammatory effects (73, 74). Furthermore, Annexin A1 has been positively linked upstream to the ERK/MAPK pathway, with phosphorylation of Annexin A1 associated with cell proliferation and survival (75). Annexin I has also been found to be pro-angiogenic in its ability to rescue angiogenic sprouts, although its definitive role is still unclear (74). In our data, Annexin signaling is attenuated and dampened with the introduction of PF-4. Down-regulation of Annexin can potentially lead to down-regulation of PLC group signaling and is recapitulated here in our data as a result of stimulation with PF-4 (76).

It is difficult to assess the implications involved with all the phosphosites identified in our system for proteins such as SHC1, as its family of adaptor proteins is implicated in many mechanisms including MAPK/ERK activation (77, 78). Likewise, assessment of Shp2 is difficult as characterization of phospho-Y62 has yet to be reported in literature, although Shp2 appears to play important roles in activating substrates which are negatively regulated by phosphorylation (79). Although the remaining proteins have generally been characterized for certain functions, their phosphorylation sites identified in our data set are uncharacterized to date, making their specific roles in the signaling network between VEGF and PF-4 unknown. Furthermore, because of the complexity inherent in phosphoprotein signaling pathways, as well as the large number of potential correlations observed for each of the treatment conditions in this data set, it is difficult to glean specific information about the behavior of every protein in context of another.

Despite the difficulty in dealing with large complex networks, the flowchart assembled in Fig. 5 appears to generate an interesting landscape centered on the Ephrin A2 receptor. Although EphA2 has been reported to facilitate angiogenic processes, in our system we found that EphA2 correlations increased significantly when PF-4 was simultaneously present with VEGF. In fact, many of the correlations did not appear until after PF-4 was in the system. Ephrin and its class of RTK receptors have been recognized as important regulators of embryonic vascular development (class B) and vascular remodeling of mature tissues (class A) (80, 81). In mature adult systems, EphA2 is associated with mediating vascular remodeling promoting cell migration and sprouting (82). EphA2 Y772 phosphorylation is implicated in mediating cell-cell interactions, and from initial analysis of the time course data in the context of previous studies, is required for progression of angiogenesis (80, 83).

The addition of PF-4 delayed EphA2 phosphorylation dynamics relative to VEGF treatment alone. These changes in signaling dynamics occur in tandem with FAK, Fyn, Lyn, and P38α. In fact, we also observed a number of positive correlations of EphA2 with Src family kinases and P38α, whose phosphorylation have been reported to modulate cell migration (51, 84). As a result, we speculate that PF-4 stimulates EphA2's regulatory role on cell-cell interactions to reduce the sprouting capacity of endothelial cells, or even implicate its

role in ensuring only the most robust sprouts form by preventing bulk cell invasion.

This "cohesive" behavior in which cells remain clustered together has been speculated previously for initiation of tumor metastasis and that EphA2 expression in tumor cells inhibits their propensity to migrate (85). Tumor malignancy occurs when these cells overcome this ephrin ligand inhibition, through exploitation of vasculogenic mimicry. VE-cadherin and EphA2 crosstalk has been found in melanoma vasculogenic mimicry where EphA2 colocalizes with VE-cadherin (86, 87). EphA2 has also been implicated in inhibiting integrin-mediated adhesion, migration, and signaling, thereby contributing to a potential role in negative regulation following PF-4 treatment (88). This previous finding would also agree with what we observe for signaling involved in migration; FAK decreases over time in the presence of PF-4 and is negatively regulated by EphA2. In addition, PF-4 treatments could also potentially modulate EphA2 signaling dynamics by affecting ephrinA1 presentation or expression, which can also induce reverse signaling on neighboring cells to promote bulk homeostasis or single cell migration (48, 53). However, a caveat of EphA2 signaling is that it has been implicated in many modalities of functions, often paradoxical for homeostatic systems compared with metastatic cancer models (51, 53, 82, 89). With the multiple functions that EphA2 can perform, it is clear that regulation of EphA2 is crucial, and our data suggests that its actions may be impinged or influenced by PF-4.

Despite our success with quantifying tyrosine phosphorylation signaling networks, we realize that a majority of signaling data was lost because of the inherent difficulties working with our system; a low signaling primary cell type in conjunction with a highly concentrated matrix scaffold can drown out low level signaling. This challenge was apparent in our original captured list of phosphoproteomic data; we observed over 400 different phosphorylation sites across 350 unique proteins that were significant hits. However, there was insufficient quantitation in many of these measurements because of very low level signaling. The presence of serum also introduces a high proportion of background noise into our measurements (as is observed in the error of some measurements shown in Fig. 2). To recover some of the lost quantitation, we attempted different data processing methods to increase our phosphoprotein coverage, including pooling time points into broader categories. Although we slightly increased the number of proteins that had statistical significance in temporal dynamics, it was at the expense of correlative power in our topographical analysis (data not shown).

We have developed new processing methods to explore pro- and anti-angiogenic signaling pathways in collagen gel substrates. Relatively few studies have been performed in the past on how PF-4 affects intracellular signaling in endothelial cells. Our preliminary data indicate that PF-4 primarily induces its angiostatic effects on microvascular endothelial cells via pathways that control cell migration which precede sprouting and invasion phenotype. From assessments of the time course data and correlation network modeling, we have found substantial implications of EphA2 signaling dynamics in negatively regulating cell migration and angiogenesis following stimulation, contrary to previous reports of its role in promoting cell migration and sprouting. Our work indicates EphA2 signaling as an area of interest and future focus for understanding angiostatic mechanisms.

To our knowledge, this is the first large phosphoproteomic signaling data set that has been collected from primary endothelial cells cultured in a gel system. Although far from being *in vivo* conditions, this culture system is more reflective of physiological environments encountered as opposed to standard two-dimensional cultures performed in the past. The data gathered in this project not only provides new insight about PF-4 and its interplay with VEGF on angiogenesis, but can also be used to inform behavioral models of endothelial cells (22), as well as follow-up analyses using targeted MS-based approached, such as multiple reaction monitoring, to gain increased coverage of the known and newly discovered phosphosites reported here. These findings and their applications can build a foundation for future studies of molecular interplay involved in inflammation and angiogenesis in physiologically relevant models.

Acknowledgments—We thank the White Lab and particularly Hannah Johnson, Bryan Bryson, Tim Curran, Amanda Del Rosario and Jason Neil for helpful discussions; Shannon Hughes for discussions on experimental approaches; Hsinhwa Lee for helping us secure necessary reagents and supplies in our experiments; and we would like to thank Emily Miraldi, Kristen Naegle, Melody Morris, Miles Miller, Joel Wagner, and Brian Joughin for their advice in data processing and modeling. Finally, we would like to thank Abhinav Arneja, Lorenna Buck, Sarah Kolitz, Dave Clarke, and Aaron Meyer for helpful discussions and suggestions.

* This work was supported by NSF EFRI grant 735997, NIH Cell Migration Consortium grant GM06346, NIH Cell Decision Processes Center grant GM68762, NIH grant GM69668, and NIH grant GM81336.

S This article contains Supplemental Figs. S1 and S2 and Video S1.

‖ To whom correspondence should be addressed: Department of Biological Engineering, 77 Massachusetts Avenue, Building 16 Room 343, Cambridge, MA, 02139. Tel.: 617-252-1629; Fax: 617-258-0204; E-mail: lauffen@mit.edu.

¶ These authors contributed equally.

Author contributions: TCH, NCT, RJR, and TR did the experiments. TCH, NCT, RJR, AW, FMW, RDK, and DAL contributed to design, interpretation, and troubleshooting of experiments. TCH wrote the paper with assistance from NCT and DAL.

REFERENCES

1. Carmeliet, P. (2005) Angiogenesis in life, disease and medicine. *Nature* **438,** 932–936
2. Saharinen, P., Eklund, L., Miettinen, J., Wirkkala, R., Anisimov, A., Winderlich, M., Nottebaum, A., Vestweber, D., Deutsch, U., Koh, G. Y., Olsen, B. R., and Alitalo, K. (2008) Angiopoietins assemble distinct Tie2 signalling complexes in endothelial cell-cell and cell-matrix contacts. *Nat. Cell Biol.* **10,** 527–537
3. Singh, R., Kaushik, S., Wang, Y., Xiang, Y., Novak, I., Komatsu, M., Tanaka, K., Cuervo, A. M., and Czaja, M. J. (2009) Autophagy regulates lipid metabolism. *Nature* **458,** 1131–1135

4. Adair, T. H., and Montani, J.-P. (2010) Angiogenesis, Morgan & Claypool Life Sciences, San Rafael, CA.
5. Yancopoulos, G. D., Davis, S., Gale, N. W., Rudge, J. S., Wiegand, S. J., and Holash, J. (2000) Vascular-specific growth factors and blood vessel formation. *Nature* **407,** 242–248
6. Barrientos, S., Stojadinovic, O., Golinko, M. S., Brem, H., and Tomic-Canic, M. (2008) Growth factors and cytokines in wound healing. *Wound Repair Regen.* **16,** 585–601
7. Gillitzer, R., and Goebeler, M. (2001) Chemokines in cutaneous wound healing. *J. Leukoc. Biol.* **69,** 513–521
8. Werner, S., and Grose, R. (2003) Regulation of wound healing by growth factors and cytokines. *Physiol. Rev.* **83,** 835–870
9. Kobayashi, H., and Lin, P. C. (2009) Angiogenesis links chronic inflammation with cancer. *Methods Mol. Biol.* **511,** 185–191
10. Szekanecz, Z., and Koch, A. E. (2004) Vascular endothelium and immune responses: implications for inflammation and angiogenesis. *Rheum. Dis. Clin. North Am.* **30,** 97–114
11. Kundu, J. K., and Surh, Y.-J. (2008) Inflammation: gearing the journey to cancer. *Mutat. Res.* **659,** 15–30
12. Carmeliet, P., and Jain, R. K. (2011) Molecular mechanisms and clinical applications of angiogenesis. *Nature* **473,** 298–307
13. Sahota, P. S., Burn, J. L., Brown, N. J., and MacNeil, S. (2004) Approaches to improve angiogenesis in tissue-engineered skin. *Wound Repair Regen.* **12,** 635–642
14. Feil, G., Daum, L., Amend, B., Maurer, S., Renninger, M., Vaegler, M., Seibold, J., Stenzl, A., and Sievert, K.-D. (2011) From tissue engineering to regenerative medicine in urology–the potential and the pitfalls. *Adv. Drug Deliv. Rev.* **63,** 375–378
15. Sherwood, J. K., Riley, S. L., Palazzolo, R., Brown, S. C., Monkhouse, D. C., Coates, M., Griffith, L. G., Landeen, L. K., and Ratcliffe, A. (2002) A three-dimensional osteochondral composite scaffold for articular cartilage repair. *Biomaterials* **23,** 4739–4751
16. Ban, D.-X., Kong, X.-H., Feng, S.-Q., Ning, G.-Z., Chen, J.-T., and Guo, S.-F. (2009) Intraspinal cord graft of autologous activated Schwann cells efficiently promotes axonal regeneration and functional recovery after rat's spinal cord injury. *Brain Res.* **1256,** 149–161
17. Hu, X., Huang, J., Ye, Z., Xia, L., Li, M., Lv, B., Shen, X., and Luo, Z. (2009) A novel scaffold with longitudinally oriented microchannels promotes peripheral nerve regeneration., *Tissue Eng.* **15,** 3297–3308
18. Kaully, T., Kaufman-Francis, K., Lesman, A., and Levenberg, S. (2009) Vascularization–the conduit to viable engineered tissues. *Tissue Eng.* **15,** 159–169
19. Soker, S., Machado, M., and Atala, A. (2000) Systems for therapeutic angiogenesis in tissue engineering. *World J. Urol.* **18,** 10–18
20. Kirkpatrick, C. J., Otto, M., Van Kooten, T., Krump, V., Kriegsmann, J., and Bittinger, F. (1999) Endothelial cell cultures as a tool in biomaterial research. *J. Mater. Sci. Mater. Med.* **10,** 589–594
21. Mendes, J. B., Campos, P. P., Ferreira, M. A. N. D., Bakhle, Y. S., and Andrade, S. P. (2007) Host response to sponge implants differs between subcutaneous and intraperitoneal sites in mice. *J. Biomed. Mater. Res.* **83,** 408–415
22. Rimchala, T., Kamm, R. D., and Lauffenburger, D. A. (2013) Endothelial cell phenotypic behaviors cluster into dynamic state transition programs modulated by angiogenic and angiostatic cytokines. *Integr. Biol.* **5,** 510–522
23. Bernardini, G., Ribatti, D., Spinetti, G., Morbidelli, L., Ziche, M., Santoni, A., Capogrossi, M. C., and Napolitano, M. (2003) Analysis of the role of chemokines in angiogenesis. *J. Immunol. Methods* **273,** 83–101
24. Keeley, E. C., Mehrad, B., and Strieter, R. M. (2008) Chemokines as mediators of neovascularization. *Arteriosclerosis, Thrombosis, Vasc. Biol.* **28,** 1928–1936
25. Mehrad, B., Keane, M. P., and Strieter, R. M. (2007) Chemokines as mediators of angiogenesis. *Thromb. Haemost.* **97,** 755–762
26. Rosenkilde, M. M., and Schwartz, T. W. (2004) The chemokine system – a major regulator of angiogenesis in health and disease. *APMIS* **112,** 481–495
27. Slungaard, A. (2005) Platelet factor 4: a chemokine enigma. *Int. J. Biochem. Cell Biol.* **37,** 1162–1167
28. Aidoudi, S., and Bikfalvi, A. (2010) Interaction of PF4 (CXCL4) with the vasculature: a role in atherosclerosis and angiogenesis. *Thromb. Haemost.* **104,** 941–948
29. Vandercappellen, J., Van Damme, J., and Struyf, S. (2011) The role of the CXC chemokines platelet factor-4 (CXCL4/PF-4) and its variant (CXCL4L1/PF-4var) in inflammation, angiogenesis and cancer. *Cytokine Growth Factor Rev.* **22,** 1–18
30. Vandercappellen, J., Van Damme, J., and Struyf, S. (2008) The role of CXC chemokines and their receptors in cancer. *Cancer Letters* **267,** 226–244
31. Shao, X. J., and Xie, F. M. (2005) Influence of angiogenesis inhibitors, endostatin and PF-4, on lymphangiogenesis. *Lymphology* **38,** 1–8
32. Gupta, S. K., and Singh, J. P. (1994) Inhibition of endothelial cell proliferation by platelet factor-4 involves a unique action on S phase progression. *J. Cell Biol.* **127,** 1121–1127
33. Sulpice, E., Contreres, J.-O., Lacour, J., Bryckaert, M., and Tobelem, G. (2004) Platelet factor 4 disrupts the intracellular signalling cascade induced by vascular endothelial growth factor by both KDR dependent and independent mechanisms. *Eur. J. Biochem.* **271,** 3310–3318
34. Tabruyn, S. P., and Griffioen, A. W. (2007) Molecular pathways of angiogenesis inhibition. *Biochem. Biophys. Res. Commun.* **355,** 1–5
35. Petrai, I., Rombouts, K., Lasagni, L., Annunziato, F., Cosmi, L., Romanelli, R. G., Sagrinati, C., Mazzinghi, B., Pinzani, M., Romagnani, S., Romagnani, P., and Marra, F. (2008) Activation of p38(MAPK) mediates the angiostatic effect of the chemokine receptor CXCR3-B. *Int. J. Biochem. Cell Biol.* **40,** 1764–1774
36. Bodnar, R. J., Yates, C. C., and Wells, A. (2006) IP-10 blocks vascular endothelial growth factor-induced endothelial cell motility and tube formation via inhibition of calpain. *Circulation Res.* **98,** 617–625
37. Bodnar, R. J., Yates, C. C., Rodgers, M. E., Du, X., and Wells, A. (2009) IP-10 induces dissociation of newly formed blood vessels. *J. Cell Sci.* **122,** 2064–2077
38. Salcedo, R., Resau, J. H., Halverson, D., Hudson, E. A., Dambach, M., Powell, D., Wasserman, K., and Oppenheim, J. J. (2000) Differential expression and responsiveness of chemokine receptors (CXCR1–3) by human microvascular endothelial cells and umbilical vein endothelial cells. *FASEB J.* **14,** 2055–2064
39. Chung, S., Sudo, R., Zervantonakis, I. K., Rimchala, T., and Kamm, R. D. (2009) Surface-treatment-induced three-dimensional capillary morphogenesis in a microfluidic platform., *Adv. Mater. Weinheim* **21,** 4863–4867
40. Shults, M. D., Janes, K. A., Lauffenburger, D. A., and Imperiali, B. (2005) A multiplexed homogeneous fluorescence-based assay for protein kinase activity in cell lysates. *Nat. Methods* **2,** 277–283
41. Zhang, Y., Wolf-Yadlin, A., and White, F. M. (2007) Quantitative proteomic analysis of phosphotyrosine-mediated cellular signaling networks. *Methods Mol. Biol.* **359,** 203–212
42. Spangler, J. B., Neil, J. R., Abramovitch, S., Yarden, Y., White, F. M., Lauffenburger, D. A., and Wittrup, K. D. (2010) Combination antibody treatment down-regulates epidermal growth factor receptor by inhibiting endosomal recycling. *Proc. Natl. Acad. Sci. U.S.A.* **107,** 13252–13257
43. Mortensen, P., Gouw, J. W., Olsen, J. V., Ong, S.-E., Rigbolt, K. T. G., Bunkenborg, J., Cox, J., Foster, L. J., Heck, A. J. R., Blagoev, B., Andersen, J. S., and Mann, M. (2010) MSQuant, an open source platform for mass spectrometry-based quantitative proteomics. *J. Proteome Res.* **9,** 393–403
44. Perkins, D. N., Pappin, D. J., Creasy, D. M., and Cottrell, J. S. (1999) Probability-based protein identification by searching sequence databases using mass spectrometry data. *Electrophoresis* **20,** 3551–3567
45. Nichols, A. M., and White, F. M. (2009) Manual validation of peptide sequence and sites of tyrosine phosphorylation from MS/MS spectra. *Methods Mol. Biol.* **492,** 143–160
46. Naegle, K. M., Gymrek, M., Joughin, B. A., Wagner, J. P., Welsch, R. E., Yaffe, M. B., Lauffenburger, D. A., and White, F. M. (2010) PTMScout, a Web resource for analysis of high throughput post-translational proteomics studies. *Mol. Cell Proteomics* **9,** 2558–2570
47. Kim, H.-D., Meyer, A. S., Wagner, J. P., Alford, S. K., Wells, A., Gertler, F. B., and Lauffenburger, D. A. (2011) Signaling network state predicts twist-mediated effects on breast cell migration across diverse growth factor contexts. *Mol. Cell Proteomics* 10, M111.008433
48. Wykosky, J., Palma, E., Gibo, D. M., Ringler, S., Turner, C. P., and Debinski, W. (2008) Soluble monomeric EphrinA1 is released from tumor cells and is a functional ligand for the EphA2 receptor. *Oncogene* **27,** 7260–7273

49. Miao, H., Li, D.-Q., Mukherjee, A., Guo, H., Petty, A., Cutter, J., Basilion, J. P., Sedor, J., Wu, J., Danielpour, D., Sloan, A. E., Cohen, M. L., and Wang, B. (2009) EphA2 mediates ligand-dependent inhibition and ligand-independent promotion of cell migration and invasion via a reciprocal regulatory loop with Akt. *Cancer Cell* **16,** 9–20
50. Walker-Daniels, J., Riese, D. J., and Kinch, M. S. (2002) c-Cbl-dependent EphA2 protein degradation is induced by ligand binding. *Mol. Cancer Res.* **1,** 79–87
51. Pasquale, E. B. (2010) Eph receptors and ephrins in cancer: bidirectional signalling and beyond. *Nat. Rev. Cancer* **10,** 165–180
52. Kikawa, K. D., Vidale, D. R., Van Etten, R. L., and Kinch, M. S. (2002) Regulation of the EphA2 kinase by the low molecular weight tyrosine phosphatase induces transformation. *J. Biol. Chem.* **277,** 39274–39279
53. Beauchamp, A., and Debinski, W. (2012) Ephs and ephrins in cancer: Ephrin-A1 signalling. *Semin. Cell Develop. Biol.* **23,** 109–115
54. Noberini, R., Koolpe, M., Peddibhotla, S., Dahl, R., Su, Y., Cosford, N. D. P., Roth, G. P., and Pasquale, E. B. (2008) Small molecules can selectively inhibit ephrin binding to the EphA4 and EphA2 receptors. *J. Biol. Chem.* **283,** 29461–29472
55. Noberini, R., Lamberto, I., and Pasquale, E. B. (2011) Targeting Eph receptors with peptides and small molecules: Progress and challenges. *Semin. Cell Develop. Biol.* **23,** 51–57
56. Dephoure, N., Zhou, C., Villén, J., Beausoleil, S. A., Bakalarski, C. E., Elledge, S. J., and Gygi, S. P. (2008) A quantitative atlas of mitotic phosphorylation. *Proc. Natl. Acad. Sci. U.S.A.* **105,** 10762–10767
57. Platt, M. O., Wilder, C. L., Wells, A., Griffith, L. G., and Lauffenburger, D. A. (2009) Multipathway kinase signatures of multipotent stromal cells are predictive for osteogenic differentiation: tissue-specific stem cells. *Stem Cells* **27,** 2804–2814
58. Kanaji, N., Nelson, A., Allen-Gipson, D. S., Sato, T., Nakanishi, M., Wang, X., Li, Y., Basma, H., Michalski, J., Farid, M., Rennard, S. I., and Liu, X. (2012) The p38 mitogen-activated protein kinases modulate endothelial cell survival and tissue repair. *Inflamm. Res.* **61,** 233–244
59. Raingeaud, J., Gupta, S., Rogers, J. S., Dickens, M., Han, J., Ulevitch, R. J., and Davis, R. J. (1995) Pro-inflammatory cytokines and environmental stress cause p38 mitogen-activated protein kinase activation by dual phosphorylation on tyrosine and threonine. *J. Biol. Chem.* **270,** 7420–7426
60. Roux, P. P., and Blenis, J. (2004) ERK and p38 MAPK-activated protein kinases: a family of protein kinases with diverse biological functions. *Microbiol. Mol. Biol. Rev.* **68,** 320–344
61. Zhang, Y.-Y., Mei, Z.-Q., Wu, J.-W., and Wang, Z.-X. (2008) Enzymatic activity and substrate specificity of mitogen-activated protein kinase p38alpha in different phosphorylation states. *J. Biol. Chem.* **283,** 26591–26601
62. Werdich, X. Q., and Penn, J. S. (2005) Src, Fyn and Yes play differential roles in VEGF-mediated endothelial cell events. *Angiogenesis* **8,** 315–326
63. Zhao, X., and Guan, J.-L. (2011) Focal adhesion kinase and its signaling pathways in cell migration and angiogenesis. *Adv. Drug Deliv. Rev.* **63,** 610–615
64. Calalb, M. B., Polte, T. R., and Hanks, S. K. (1995) Tyrosine phosphorylation of focal adhesion kinase at sites in the catalytic domain regulates kinase activity: a role for Src family kinases. *Mol. Cell. Biol.* **15,** 954–963
65. Matsui, H., Harada, I., and Sawada, Y. (2012) Src, p130Cas, and mechanotransduction in cancer cells. *Genes Cancer* **3,** 394–401
66. Kawauchi, K., Tan, W. W., Araki, K., Abu Bakar, F. B., Kim, M., Fujita, H., Hirata, H., and Sawada, Y. (2012) p130Cas-dependent actin remodelling regulates myogenic differentiation. *Biochem. J.* **445,** 323–332
67. George, B., Verma, R., Soofi, A. A., Garg, P., Zhang, J., Park, T.-J., Giardino, L., Ryzhova, L., Johnstone, D. B., Wong, H., Nihalani, D., Salant, D. J., Hanks, S. K., Curran, T., Rastaldi, M. P., and Holzman, L. B. (2012) Crk1/2-dependent signaling is necessary for podocyte foot process spreading in mouse models of glomerular disease. *J. Clin. Invest.* **122,** 674–692
68. Liu, G., Place, A. T., Chen, Z., Brovkovych, V. M., Vogel, S. M., Muller, W. A., Skidgel, R. A., Malik, A. B., and Minshall, R. D. (2012) ICAM-1-activated Src and eNOS signaling increase endothelial cell surface PECAM-1 adhesivity and neutrophil transmigration. *Blood* **120,** 1942–1952
69. Fujiwara, K., Masuda, M., Osawa, M., Kano, Y., and Katoh, K. (2001) Is PECAM-1 a mechanoresponsive molecule? *Cell Struct. Funct.* **26,** 11–17
70. Newman, P. J., and Newman, D. K. (2003) Signal transduction pathways mediated by PECAM-1: new roles for an old molecule in platelet and vascular cell biology. *Arterioscler Thromb Vasc Biol.* **23,** 953–964
71. Jackson, D. E. (2003) The unfolding tale of PECAM-1. *FEBS Lett.* **540,** 7–14
72. Chiu, Y.-J., McBeath, E., and Fujiwara, K. (2008) Mechanotransduction in an extracted cell model: Fyn drives stretch- and flow-elicited PECAM-1 phosphorylation. *J. Cell Biol.* **182,** 753–763
73. Perretti, M., and Dalli, J. (2009) Exploiting the Annexin A1 pathway for the development of novel anti-inflammatory therapeutics. *Br. J. Pharmacol.* **158,** 936–946
74. Yi, M., and Schnitzer, J. E. (2009) Impaired tumor growth, metastasis, angiogenesis and wound healing in annexin A1-null mice., *Proc. Natl. Acad. Sci. U.S.A.* **106,** 17886–17891
75. Lim, L. H. K., and Pervaiz, S. (2007) Annexin 1: the new face of an old molecule. *FASEB J.* **21,** 968–975
76. Frey, B. M., Reber, B. F., Vishwanath, B. S., Escher, G., and Frey, F. J. (1999) Annexin I modulates cell functions by controlling intracellular calcium release. *FASEB J.* **13,** 2235–2245
77. Vindis, C., Cerretti, D. P., Daniel, T. O., and Huynh-Do, U. (2003) EphB1 recruits c-Src and p52Shc to activate MAPK/ERK and promote chemotaxis. *J. Cell Biol.* **162,** 661–671
78. Ravichandran, K. S. (2001) Signaling via Shc family adapter proteins. *Oncogene* **20,** 6322–6330
79. Matozaki, T., Murata, Y., Saito, Y., Okazawa, H., and Ohnishi, H. (2009) Protein tyrosine phosphatase SHP-2: a proto-oncogene product that promotes Ras activation. *Cancer Sci.* **100,** 1786–1793
80. Brantley-Sieders, D. M., Caughron, J., Hicks, D., Pozzi, A., Ruiz, J. C., and Chen, J. (2004) EphA2 receptor tyrosine kinase regulates endothelial cell migration and vascular assembly through phosphoinositide 3-kinase-mediated Rac1 GTPase activation. *J. Cell Sci.* **117,** 2037–2049
81. Campbell, T. N., and Robbins, S. M. (2008) The Eph receptor/ephrin system: an emerging player in the invasion game. *Curr. Issues Mol. Biol.* **10,** 61–66
82. Poliakov, A., Cotrina, M., and Wilkinson, D. G. (2004) Diverse roles of eph receptors and ephrins in the regulation of cell migration and tissue assembly. *Dev. Cell* **7,** 465–480
83. Cheng, N., Brantley, D. M., Liu, H., Lin, Q., Enriquez, M., Gale, N., Yancopoulos, G., Cerretti, D. P., Daniel, T. O., and Chen, J. (2002) Blockade of EphA receptor tyrosine kinase activation inhibits vascular endothelial cell growth factor-induced angiogenesis. *Mol. Cancer Res.* **1,** 2–11
84. Kasper, B., and Petersen, F. (2011) Molecular pathways of platelet factor 4/CXCL4 signaling. *Eur. J. Cell Biol.* **90,** 521–526
85. Larsen, A. B., Pedersen, M. W., Stockhausen, M.-T., Grandal, M. V., van Deurs, B., and Poulsen, H. S. (2007) Activation of the EGFR gene target EphA2 inhibits epidermal growth factor-induced cancer cell motility. *Mol. Cancer Res.* **5,** 283–293
86. Hendrix, M. J. C., Seftor, E. A., Hess, A. R., and Seftor, R. E. B. (2003) Vasculogenic mimicry and tumour-cell plasticity: lessons from melanoma. *Nat Rev Cancer* **3,** 411–421
87. Hess, A. R., Seftor, E. A., Gruman, L. M., Kinch, M. S., Seftor, R. E. B., and Hendrix, M. J. C. (2006) VE-cadherin regulates EphA2 in aggressive melanoma cells through a novel signaling pathway: implications for vasculogenic mimicry. *Cancer Biol. Ther.* **5,** 228–233
88. Miao, H., Burnett, E., Kinch, M., Simon, E., and Wang, B. (2000) Activation of EphA2 kinase suppresses integrin function and causes focal-adhesion-kinase dephosphorylation. *Nat Cell Biol.* **2,** 62–69
89. Miao, H., and Wang, B. (2012) EphA receptor signaling-Complexity and emerging themes. *Semin. Cell Develop. Biol.* **23,** 16–25
90. Radke, S., Austermann, J., Russo-Marie, F., Gerke, V., and Rescher, U. (2004) Specific association of annexin 1 with plasma membrane-resident and internalized EGF receptors mediated through the protein core domain. *FEBS Lett.* **578,** 95–98
91. Tcatchoff, L., Andersson, S., Utskarpen, A., Klokk, T. I., Skånland, S. S., Pust, S., Gerke, V., and Sandvig, K. (2012) Annexin A1 and A2: roles in retrograde trafficking of Shiga toxin. *PLoS ONE* **7,** e40429
92. Anastasiadis, P. Z., and Reynolds, A. B. (2000) The p120 catenin family: complex roles in adhesion, signaling and cancer. *J. Cell Sci.* **113,** 1319–1334

93. Hu, G. (2012) p120-Catenin: a novel regulator of innate immunity and inflammation. *Crit. Rev. Immunol.* **32,** 127–138
94. Potapova, T. A., Daum, J. R., Byrd, K. S., and Gorbsky, G. J. (2009) Fine tuning the cell cycle: activation of the Cdk1 inhibitory phosphorylation pathway during mitotic exit. *Mol. Biol. Cell* **20,** 1737–1748
95. Welburn, J. P. I., Tucker, J. A., Johnson, T., Lindert, L., Morgan, M., Willis, A., Noble, M. E. M., and Endicott, J. A. (2007) How tyrosine 15 phosphorylation inhibits the activity of cyclin-dependent kinase 2-cyclin A. *J. Biol. Chem.* **282,** 3173–3181
96. Squire, C. J., Dickson, J. M., Ivanovic, I., and Baker, E. N. (2005) Structure and inhibition of the human cell cycle checkpoint kinase, Wee1A kinase: an atypical tyrosine kinase with a key role in CDK1 regulation. *Structure* **13,** 541–550
97. Mayya, V., Rezual, K., Wu, L., Fong, M. B., and Han, D. K. (2006) Absolute quantification of multisite phosphorylation by selective reaction monitoring mass spectrometry: determination of inhibitory phosphorylation status of cyclin-dependent kinases. *Mol. Cell. Proteomics* **5,** 1146–1157
98. Norbury, C., Blow, J., and Nurse, P. (1991) Regulatory phosphorylation of the p34cdc2 protein kinase in vertebrates. *EMBO J.* **10,** 3321–3329
99. Lee, K., Deng, X., and Friedman, E. (2000) Mirk protein kinase is a mitogen-activated protein kinase substrate that mediates survival of colon cancer cells. *Cancer Res.* **60,** 3631–3637
100. Fang, W. B., Brantley-Sieders, D. M., Hwang, Y., Ham, A.-J. L., and Chen, J. (2008) Identification and functional analysis of phosphorylated tyrosine residues within EphA2 receptor tyrosine kinase. *J. Biol. Chem.* **283,** 16017–16026
101. Balasubramaniam, D., Paul, L. N., Homan, K. T., Hall, M. C., and Stauffacher, C. V. (2011) Specificity of HCPTP variants toward EphA2 tyrosines by quantitative selected reaction monitoring. *Protein Sci.* **20,** 1172–1181
102. Thalhammer, A., Trinidad, J. C., Burlingame, A. L., and Schoepfer, R. (2009) Densin-180: revised membrane topology, domain structure and phosphorylation status. *J. Neurochem.* **109,** 297–302
103. Eminaga, S., and Bennett, A. M. (2008) Noonan syndrome-associated SHP-2/Ptpn11 mutants enhance SIRPalpha and PZR tyrosyl phosphorylation and promote adhesion-mediated ERK activation. *J. Biol. Chem.* **283,** 15328–15338
104. Romanova, L. Y., Hashimoto, S., Chay, K.-O., Blagosklonny, M. V., Sabe, H., and Mushinski, J. F. (2004) Phosphorylation of paxillin tyrosines 31 and 118 controls polarization and motility of lymphoid cells and is PMA-sensitive. *J. Cell Sci.* **117,** 3759–3768
105. Tsubouchi, A., Sakakura, J., Yagi, R., Mazaki, Y., Schaefer, E., Yano, H., and Sabe, H. (2002) Localized suppression of RhoA activity by Tyr31/118-phosphorylated paxillin in cell adhesion and migration. *J. Cell Biol.* **159,** 673–683
106. Ren, Y., Chen, Z., Chen, L., Fang, B., Win-Piazza, H., Haura, E., Koomen, J. M., and Wu, J. (2010) Critical role of Shp2 in tumor growth involving regulation of c-Myc. *Genes Cancer* **1,** 994–1007
107. Huang, P. H., Mukasa, A., Bonavia, R., Flynn, R. A., Brewer, Z. E., Cavenee, W. K., Furnari, F. B., and White, F. M. (2007) Quantitative analysis of EGFRvIII cellular signaling networks reveals a combinatorial therapeutic strategy for glioblastoma. *Proc. Natl. Acad. Sci. U.S.A.* **104,** 12867–12872
108. Su, J., Yang, L. T., and Sap, J. (1996) Association between receptor protein-tyrosine phosphatase RPTPalpha and the Grb2 adaptor. Dual Src homology (SH) 2/SH3 domain requirement and functional consequences. *J. Biol. Chem.* **271,** 28086–28096
109. Tremper-Wells, B., Resnick, R. J., Zheng, X., Holsinger, L. J., and Shalloway, D. (2010) Extracellular domain dependence of PTPalpha transforming activity. *Genes Cells* **15,** 711–724
110. O'Meara, R. W., Michalski, J.-P., and Kothary, R. (2011) Integrin signaling in oligodendrocytes and its importance in CNS myelination. *J. Signal Transduct.* 2011:354091
111. Shikata, Y., Birukov, K. G., Birukova, A. A., Verin, A., and Garcia, J. G. N. (2003) Involvement of site-specific FAK phosphorylation in sphingosine-1 phosphate- and thrombin-induced focal adhesion remodeling: role of Src and GIT. *FASEB J.* **17,** 2240–2249
112. Patrussi, L., Ulivieri, C., Lucherini, O. M., Paccani, S. R., Gamberucci, A., Lanfrancone, L., Pelicci, P. G., and Baldari, C. T. (2007) p52Shc is required for CXCR4-dependent signaling and chemotaxis in T cells. *Blood* **110,** 1730–1738
113. Sotirellis, N., Johnson, T. M., Hibbs, M. L., Stanley, I. J., Stanley, E., Dunn, A. R., and Cheng, H. C. (1995) Autophosphorylation induces autoactivation and a decrease in the Src homology 2 domain accessibility of the Lyn protein kinase. *J. Biol. Chem.* **270,** 29773–29780
114. Vizcaíno, J. A., Côté, R. G., Csordas, A., Dianes, J. A., Fabregat, A., Foster, J. M., Griss, J., Alpi, E., Birim, M., Contell, J., O'Kelly, G., Schoenegger, A., Ovelleiro, D., Pérez-Riverol, Y., Reisinger, F., Ríos, D., Wang, R., and Hermjakob, H. (2013) The PRoteomics IDEntifications (PRIDE) database and associated tools: status in 2013. *Nucleic Acids Res.* **41,** D1063–D1069